

## **General Disclaimer**

### **One or more of the Following Statements may affect this Document**

- This document has been reproduced from the best copy furnished by the organizational source. It is being released in the interest of making available as much information as possible.
- This document may contain data, which exceeds the sheet parameters. It was furnished in this condition by the organizational source and is the best copy available.
- This document may contain tone-on-tone or color graphs, charts and/or pictures, which have been reproduced in black and white.
- This document is paginated as submitted by the original source.
- Portions of this document are not fully legible due to the historical nature of some of the material. However, it is the best reproduction available from the original submission.

NASA TM X- 70969

# **ANALYSES OF THE SOLID EARTH AND OCEAN TIDAL PERTURBATIONS ON THE ORBITS OF THE GEOS-I AND GEOS-II SATELLITES**

(NASA-TM-X-70969) ANALYSES OF THE SOLID  
EARTH AND OCEAN TIDAL PERTURBATIONS ON THE  
ORBITS OF THE GEOS-1 AND GEOS-2 SATELLITES  
(NASA) 33 p HC \$3.75

N75-32145

CSCS 22A

G3/13

Unclas  
40518

**T. L. FELSENTRER**

**J. G. MARSH**

**R. W. AGREEN**

JULY 1975



**GODDARD SPACE FLIGHT CENTER**  
**GREENBELT, MARYLAND**

ANALYSES OF THE SOLID EARTH AND OCEAN TIDAL  
PERTURBATIONS ON THE ORBITS OF THE  
GEOS-I AND GEOS-II SATELLITES

T. L. Felsentreger  
J. G. Marsh  
R. W. Agreen

July 1975

GODDARD SPACE FLIGHT CENTER  
Greenbelt, Maryland

ANALYSES OF THE SOLID EARTH AND OCEAN TIDAL  
PERTURBATIONS ON THE ORBITS OF THE  
GEOS-I AND GEOS-II SATELLITES

T. L. Felsentreger  
J. G. Marsh  
R. W. Agreen

ABSTRACT

The luni-solar tidal perturbations in the inclination of the GEOS-I and GEOS-II satellite orbits have been analyzed for the solid Earth and ocean tide contributions. Precision reduced camera and TRANET Doppler observations spanning periods of over 600 days for each satellite were used to derive mean orbital elements. Perturbations due to the earth's gravity field, solar radiation pressure, and atmospheric drag were modelled, and the resulting inclination residuals were analyzed for tidal effects. The amplitudes of the observed total tidal effects were about 1.2 arc seconds (36 meters) in the inclination of GEOS-I and 4.5 arc seconds (135 meters) for GEOS-II. The solid Earth tides were then modelled using the value for the  $k_2$  Love number of 0.30 available from Earth tide measurements, Earth rotation observations, and seismic data. The resulting inclination

residuals were then analyzed for  $K_1$ ,  $S_2$ , and  $P_1$  ocean tide parameters. Since these ocean tidal constituents produce satellite orbital perturbations with distinctly different periods (ranging from 55 to 630 days), good separation of the constituent effects was possible.

After the solution for these parameters, the inclination rms residuals were on the order of 0.1 arc seconds (about 3 meters). The satellite derived results for the  $K_1$  and  $S_2$  ocean tide parameters are in good agreement with each other and with those deduced from existing surface data models; surface data models for the  $P_1$  tide were not available for comparison. The derived parameters consist of one second degree coefficient and an accompanying phase angle in a spherical harmonic expansion of the ocean tide potential for each tidal constituent -- the results are as follows:

Tidal Constituent	Coefficient (cm.)		Phase	
	GEOS-I	GEOS-II	GEOS-I	GEOS-II
$S_2$	$C_{22} = 1.7 \pm 0.5$	$1.0 \pm 0.2$	$\epsilon_{22} = 350^\circ \pm 21^\circ$	$62^\circ \pm 11^\circ$
$K_1$	$C_{21} = 8.8 \pm 0.7$	$5.7 \pm 1.6$	$\epsilon_{21} = 15^\circ \pm 4^\circ$	$334^\circ \pm 15^\circ$
$P_1$	$C_{21} = 5.0 \pm 1.1$	$4.9 \pm 1.1$	$\epsilon_{21} = 178^\circ \pm 15^\circ$	$127^\circ \pm 12^\circ$

## CONTENTS

	<u>Page</u>
INTRODUCTION . . . . .	1
TIDAL PERTURBATION EQUATIONS . . . . .	3
COMPUTATIONAL PROCEDURES . . . . .	7
RESULTS AND CONCLUSIONS . . . . .	11
ACKNOWLEDGMENT . . . . .	15
REFERENCES . . . . .	16

## ILLUSTRATIONS

<u>Figure</u>		<u>Page</u>
1	Perturbation of the GEOS-I Orbit Caused by Solid Earth and Ocean Tides . . . . .	20
2	Perturbation of the GEOS-II Orbit Caused by Solid Earth and Ocean Tides . . . . .	21
3	Perturbation of the GEOS-I Orbit Caused by Ocean Tides . .	22
4	Perturbation of the GEOS-II Orbit Caused by Ocean Tides . .	23
5	GEOS-I Inclination Residuals After Removal of Tidal Effects . . . . .	24
6	GEOS-II Inclination Residuals After Removal of Tidal Effects . . . . .	24

## TABLES

<u>Table</u>		<u>Page</u>
1	Ocean Tide Parameters Derived from GEOS-I and GEOS-II Satellite Observations . . . . .	25
2	Ocean Tide Parameters from Surface Measurements . . . .	26
3	Combined Ocean Tide Parameters . . . . .	26



# ANALYSES OF THE SOLID EARTH AND OCEAN TIDAL PERTURBATIONS ON THE ORBITS OF THE GEOS-I AND GEOS-II SATELLITES

## INTRODUCTION

The effects of the tidal deformations of the Earth on the orbits of close Earth satellites are readily observable as long period perturbations in the orbital elements of the satellites. This has been made possible by vastly improved tracking techniques and more accurate modelling of known perturbations such as the Earth's gravity field, lunar and solar gravity, solar radiation pressure, atmospheric drag, etc. Contributing to these tidal effects are the solid Earth, ocean, and (to a somewhat lesser extent) the atmospheric tides. However, since the same frequencies are present in the effects caused by these several contributions, any attempt to simultaneously recover parameters for them from satellite data is rather prohibitive.

Previous work involving analyses of tidal effects on satellite orbits has focussed on estimating values for the solid Earth tide Love number  $k_2$  and the associated phase lag. Early efforts were undertaken by Kozai (1965, 1968) and Newton (1965, 1968). More precise work has been done recently by Anderle (1971), Douglas et al. (1974), and Smith et al. (1973). However, the results from these investigations were satellite dependent and indicated a variance in  $k_2$  from a low of about 0.22 to a high of about 0.31, which is contradictory to strong evidence pointing towards a value for  $k_2$  of about 0.30. Attempts to

explain these discrepancies by the possible latitude dependence of the Love numbers (e.g., Kaula (1969)) have been disputed by Lambeck (1974). The most feasible explanation for these anomalous results is the neglect of the ocean tidal effects, which Kaula (1962) first indicated could be perceptible. Newton (1968) erroneously thought that these effects would almost cancel out when averaged over the whole Earth. More recently, Lambeck et al. (1974) have shown that neglect of the ocean tides could introduce errors as large as 15 % in determinations of  $k_2$  and several degrees in the associated phase angle from analysis of satellite orbit data. Furthermore, as will be shown, in some instances even the atmospheric tidal perturbations cannot be neglected in determining solid Earth and ocean tidal parameters.

In this paper, an attempt has been made to screen the solid Earth tide (and atmospheric tide) effects from satellite orbital data and analyze the resulting data for ocean tidal parameters. The rationale for this approach is based on the assumption that at least the value for the second degree solid Earth tide Love number  $k_2$  has been well established, while ocean tide models for the tidal constituents deemed to be important are either in question or do not exist at all. Study has shown that long period tidal effects are most easily observable in the angle of inclination of close Earth satellites; therefore, the present work has been limited to analysis of this orbital element only.

## TIDAL PERTURBATION EQUATIONS

The ocean tide disturbing potential at a point  $(r, \phi, \lambda)$  exterior to the Earth, including the effects of ocean loading, can be expressed in a spherical harmonic expansion as follows:

$$U = \sum_{k=0}^{\infty} \sum_{\ell=0}^k (1 + K_k') g \left( \frac{3}{2k+1} \right) \left( \frac{\rho}{\rho_{\oplus}} \right) \left( \frac{a_{\oplus}}{r} \right)^{k+1} P_k^{\ell}(\sin \phi) \cdot$$

$$\cdot \left[ (a_{k\ell} \cos \theta_n + c_{k\ell} \sin \theta_n) \cos \ell \lambda \right.$$

$$\left. + (b_{k\ell} \cos \theta_n + d_{k\ell} \sin \theta_n) \sin \ell \lambda \right] \quad (1)$$

where

$r$  = geocentric distance

$\phi$  = latitude

$\lambda$  = east longitude

$a_{\oplus}$  = mean radius of the Earth

$g$  = acceleration of gravity

$\rho$  = mean density of sea water

$\rho_{\oplus}$  = average density of the Earth

$K_k'$  = load deformation coefficient of degree  $k$

$\theta_n$  = argument corresponding to a particular tidal constituent

(Lambeck et al., 1974; McClure, 1973)

$P_k^{\ell}$  = Legendre functions

$a_{k\ell}, b_{k\ell}, c_{k\ell}, d_{k\ell}$  = harmonic coefficients

Values for the load deformation coefficients are given by Longman (1966) and Farrell (1972).

If we expand the potential of Equation 1 in terms of equatorial orbital elements of an artificial satellite, we obtain

$$U = g \frac{\rho}{\rho_\oplus} \sum_{k=0}^{\infty} \sum_{\ell=0}^k (1 + K_k') \left( \frac{3}{2k+1} \right) \left( \frac{a_\oplus}{a} \right)^{k+1} \sum_{p=0}^k F_{k\ell p}(I) G_{kpq}(e) \cdot$$

$$\left\{ \begin{array}{l} C_{k\ell}^+ \sin \left[ (k-2p) \omega + (k-2p+q) M + \ell (\Omega - \theta_g) + \sigma_n + e_{k\ell}^+ \right] \\ - C_{k\ell}^- \sin \left[ (k-2p) \omega + (k-2p+q) M + \ell (\Omega - \theta_g) - \sigma_n + e_{k\ell}^- \right] \end{array} \right\}_{k-\ell \text{ even}}$$

$$\left\{ \begin{array}{l} - C_{k\ell}^+ \cos \left[ (k-2p) \omega + (k-2p+q) M + \ell (\Omega - \theta_g) + \sigma_n + e_{k\ell}^+ \right] \\ + C_{k\ell}^- \cos \left[ (k-2p) \omega + (k-2p+q) M + \ell (\Omega - \theta_g) - \sigma_n + e_{k\ell}^- \right] \end{array} \right\}_{k-\ell \text{ odd}}$$

(2)

where

- $a$  = semi-major axis of satellite's orbit
- $I$  = angle of inclination of satellite's orbit
- $e$  = eccentricity of satellite's orbit
- $\omega$  = argument of perigee of satellite's orbit
- $M$  = mean anomaly of satellite's orbit
- $\Omega$  = longitude of ascending node of satellite's orbit
- $\theta_g$  = Greenwich mean sidereal time

$F_{klp}(I), G_{kpq}(e)$  = inclination and eccentricity functions defined by

Kaula (1966)

$\sigma_n = n \theta_g - \alpha_n$  = argument corresponding to tidal constituent

$C_{k\ell}^+, C_{k\ell}^-$  = harmonic coefficients

$e_{k\ell}^+, e_{k\ell}^-$  = phase angles

Long period perturbations, i. e., those having periods longer than one revolution of the satellite, will occur only when the coefficient of  $M$ ,  $k-2p+q$ , is 0.

In addition, perturbations having periods longer than a day will appear only when  $\theta_g$  disappears from the expression, i. e., when  $\ell = n$ , which eliminates the terms multiplied by  $C_{k\ell}^-$ . The principal perturbations occur when  $q = 0$  and  $k-2p = 0$ , so the resulting principal long period potential is

$$U_L = 'g \frac{\rho}{\rho_\oplus} \sum_{k=0}^{\infty} \sum_{\ell=0}^k (1+K_k') \left( \frac{3}{2k+1} \right) \left( \frac{a_\oplus}{a} \right)^{k+1} C_{k\ell} \sum_{p=0}^k F_{klp}(I) G_{kpq}(e) \cdot$$

$$\begin{bmatrix} \sin \\ -\cos \end{bmatrix} \begin{matrix} k-\ell \text{ even} \\ k-\ell \text{ odd} \end{matrix} (\ell \Omega - \alpha_\ell + e_{k\ell}), \quad (3)$$

where  $C_{k\ell}$  and  $e_{k\ell}$  replace  $C_{k\ell}^+$  and  $e_{k\ell}^+$ , resp. For the semidiurnal tides, the most important terms are those for which  $\ell = 2$  and  $k=2, 4, 6, \dots$

In the case of the diurnal tides, we have  $\ell = 1$  and  $k=2, 4, 6, \dots$

Substituting the expression for  $U_L$  in Equation 3 into the Lagrangian equation of motion for  $I$  and integrating under the assumption that the argument is a

linear function of time yields the following perturbation equations for I, considering only the first harmonic coefficient for each tidal constituent:

$$\begin{array}{l} \text{K}_1 \text{ tide} \\ \delta I = -\frac{9}{10} g \frac{\rho}{\rho_\oplus} (1+K_2') \left( \frac{a_\oplus}{a} \right)^3 \frac{\cos I}{na^2(1-e^2)^2} C_{21} \frac{\cos(\Omega + \pi + \epsilon_{21})}{\dot{\Omega}} \end{array} \quad (4)$$

$$\begin{array}{l} \text{S}_2 \text{ tide} \\ \delta I = -\frac{9}{5} g \frac{\rho}{\rho_\oplus} (1+K_2') \left( \frac{a_\oplus}{a} \right)^3 \frac{\sin I}{na^2(1-e^2)^2} C_{22} \frac{\sin(2\Omega - 2\lambda' + \epsilon_{22})}{2\dot{\Omega} - 2\dot{\lambda}'} \end{array} \quad (5)$$

$$\begin{array}{l} \text{P}_1 \text{ tide} \\ \delta I = -\frac{9}{10} g \frac{\rho}{\rho_\oplus} (1+K_2') \left( \frac{a_\oplus}{a} \right)^3 \frac{\cos I}{na^2(1-e^2)^2} C_{21} \frac{\cos(\Omega - 2\lambda' + \pi + \epsilon_{21})}{\dot{\Omega} - 2\dot{\lambda}'} \end{array} \quad (6)$$

where

$n$  = mean motion of satellite

$\lambda'$  = mean ecliptic longitude of the Sun

Similar expressions can be derived for any of the other ocean tide constituents; however, as will be indicated later, strong evidence for observable effects from only these three constituents was found in the GEOS-I and GEOS-II data. In addition, since only the inclination data was considered, only one harmonic coefficient for each constituent could be recovered. This coefficient would be biased by the effects of the higher order coefficients (e.g.,  $C_{41}$ ,  $C_{61}$ , . . . for the  $K_1$  tide), a fact which had to be taken into account when comparing the results with existing surface data models.

## COMPUTATIONAL PROCEDURES

Derivation of ocean tidal coefficients from the analyses of GEOS-I and GEOS-II orbital data required investigation of the orbit evolution over several hundred days. The techniques and computer programs used to efficiently and accurately analyze observational data over orbital arcs of this length are discussed in the following paragraphs.

Orbit computations were carried out with the GEODYN Orbit and Geodetic Parameter Estimation Computer Program (Martin, 1972). The program employs an 11th order Cowell numerical integration procedure. Satellite disturbing forces modeled in the program included the gravity field of the earth in the form of spherical harmonic coefficients, gravity anomalies, or surface densities, third-body gravitation, atmospheric drag, luni-solar induced solid-Earth tides, and direct solar radiation pressure. For the present analyses the GSFC GEM-1 Earth Gravity Model (Lerch, et al., 1972) in the form of spherical harmonic coefficients was used. For the lunar and solar positions required in the computation of the third-body gravitational effects, the Jet Propulsion Laboratory (JPL) ephemeris tape was used. The atmospheric density was modeled by the Jacchia model atmosphere (Jacchia, 1965, 1968, 1970, 1971).

In order to investigate the long period orbital perturbations caused by the tides, a program designated ROAD (Wagner, et al., 1974) was used. This program

effects of the solid Earth and ocean tides on the inclination. There is clearly evident an effect of about 1.2 arc seconds (36 meters) in amplitude with a period of approximately 160 days, which is precisely the period of the  $K_1$  tidal effect, a luni-solar diurnal constituent.

Figure 2 shows a similar result for the GEOS-II satellite. Here, a 651 day period (beginning March 1968) of both precision reduced camera and TRANET Doppler observations were processed in the form of two-day arcs to obtain mean orbital elements. The orbital elements derived from GEOS-II camera data were published by Douglas et al. (1973). The clearly visible effect has an amplitude of about 4.5 arc seconds (135 meters). In addition to the solid Earth and ocean tidal perturbations, however, this effect also reflects a solar atmospheric tidal perturbation with an amplitude of 0.1 arc seconds and a period of approximately 436 days.

The following rationale for analyzing the data in Figures 1 and 2 was then adopted. Parameters for both the solid Earth and ocean tides cannot be recovered simultaneously, since the same frequencies are involved in each. However, the tidal effects seen in the data are essentially of second degree and the second degree solid Earth tide Love number  $k_2$  has been fairly well established as a result of Earth tide measurements, Earth rotation observations, and seismic data, while parameters for the ocean tide constituents are not too well known. Hence, the effects of the solid Earth tides were modelled



using the value  $k_2 = .3$  and a lag angle of 0 degrees, and the remaining inclination residuals were analyzed for ocean tidal effects.

Figure 3 shows the GEOS-I inclination residuals after removal of the solid Earth tide effects. A frequency analysis performed on this data indicated the presence of perturbations having periods of 160, 25, and 56 days, which correspond to long period effects caused by the  $K_1$ ,  $P_1$ , and  $S_2$  ocean tides, respectively. A subsequent least squares fit to this data involving the perturbation Equations 4, 5, and 6 resulted in the recovery of one harmonic coefficient and phase angle for each constituent ( $C_{21}$  and  $\epsilon_{21}$  for  $K_1$  and  $P_1$ , and  $C_{22}$  and  $\epsilon_{22}$  for  $S_2$ ). Values for these coefficients and phase angles are given in Table 1. In addition, the amplitudes of the effects are given in meters (Figure 3) and arc seconds (Table 1).

Figure 4 presents a similar set of inclination residuals for GEOS-II after accounting for the solid Earth tidal effects. Also taken into account, however, is a substantial solar atmospheric tidal perturbation with a frequency about equal to that of the  $S_2$  ocean tide. The perturbation equation for this effect is very similar to Equation 5. Using the coefficient and phase angle for the  $S_2$  atmospheric tide as reported in Chapman and Lindzen (1970) -  $C_{22} = .352$  mb,  $\epsilon_{22} = 158^\circ$  - it was found that this perturbation had an amplitude of slightly less than 0.1 arc seconds. Again, a least squares fit to the data shown in Figure 4, for the  $K_1$ ,  $P_1$ , and  $S_2$  ocean tides, yielded the results given in

Table 1. The periods and amplitudes (in meters) for these effects are shown on Figure 4, while the amplitudes (in arc seconds) are presented in Table 1.

The rms of the residuals after the least squares fits shown in Figures 3 and 4 were on the order of 0.1 arc seconds for each satellite. These residuals are shown in Figures 5 and 6. Frequency analyses indicate that there are no discernible significant periodicities left in these data.

## RESULTS AND CONCLUSIONS

The coefficients and phase angles presented in Table 1 are in reasonable agreement with each other, considering the differences in the amplitudes of the various effects from the two satellites and the fact that the effects of higher order harmonics have been "lumped" into the single coefficient. This latter point makes it somewhat incorrect to compare values for the same coefficient as derived from GEOS-I and GEOS-II.

To illustrate this, let us write the perturbation equations for I considering the first two significant harmonic coefficients. They have the following form:

K<sub>1</sub> tide

$$\delta I = Q C_{21} \cos (\Omega + \pi + \epsilon_{21}) + R C_{41} \cos (\Omega + \pi + \epsilon_{41}) \quad (7)$$

S<sub>2</sub> tide

$$\delta I = S C_{22} \sin (2 \Omega - 2 \lambda' + \epsilon_{22}) + T C_{42} \sin (2 \Omega - 2 \lambda' + \epsilon_{42}) \quad (8)$$

where

$$Q = -\frac{9}{10} g \frac{\rho}{\rho_{\oplus}} (1+K_2') \left( \frac{a_{\oplus}}{a} \right)^3 \frac{\cos I}{na^2 (1-e^2)^2} \frac{1}{\dot{\Omega}} \quad (9)$$

$$R = -\frac{15}{16} g \frac{\rho}{\rho_{\oplus}} (1+K_4') \left( \frac{a_{\oplus}}{a} \right)^5 \frac{\cos I (4-7 \cos^2 I) (1+3/2 e^2)}{na^2 (1-e^2)^4} \frac{1}{\dot{\Omega}} \quad (10)$$

$$S = -\frac{9}{5} g \frac{\rho}{\rho_{\oplus}} (1+K_2') \left( \frac{a_{\oplus}}{a} \right)^3 \frac{\sin I}{na^2 (1-e^2)^2} \frac{1}{2 \dot{\Omega} - 2 \dot{\lambda}'} \quad (11)$$

$$T = -\frac{5}{8} g \frac{\rho}{\rho_{\oplus}} (1+K_4') \left( \frac{a_{\oplus}}{a} \right)^5 \frac{\sin I (3-21 \cos^2 I) (1+3/2 e^2)}{na^2 (1-e^2)^4} \frac{1}{2 \dot{\Omega} - 2 \dot{\lambda}'} \quad (12)$$

Equation 7 can be rewritten as

$$\delta I = \left[ QC_{21} \cos \epsilon_{21} + RC_{41} \cos \epsilon_{41} \right] \cos (\Omega + \pi) - \left[ QC_{21} \sin \epsilon_{21} + RC_{41} \sin \epsilon_{41} \right] \cdot \sin (\Omega + \pi) \quad (13)$$

or

$$\begin{aligned} \delta I &= V \hat{C}_{21} \cos \hat{\epsilon}_{21} \cos (\Omega + \pi) - V \hat{C}_{21} \sin \hat{\epsilon}_{21} \sin (\Omega + \pi) \\ &= V \hat{C}_{21} \cos (\Omega + \pi + \hat{\epsilon}_{21}), \end{aligned} \quad (14)$$

which is of the same form as Equation 4. Similarly, for Equation 8,

$$\begin{aligned} \delta I &= \left[ SC_{22} \cos \epsilon_{22} + TC_{42} \cos \epsilon_{42} \right] \sin (2 \Omega - 2 \lambda') + \left[ SC_{22} \sin \epsilon_{22} + TC_{42} \cdot \right. \\ &\quad \left. \cdot \sin \epsilon_{42} \right] \cos (2 \Omega - 2 \lambda') \\ &= W \hat{C}_{22} \cos \hat{\epsilon}_{22} \sin (2 \Omega - 2 \lambda') + W \hat{C}_{22} \sin \hat{\epsilon}_{22} \cos (2 \Omega - 2 \lambda') \\ &= W \hat{C}_{22} \sin (2 \Omega - 2 \lambda' + \hat{\epsilon}_{22}), \end{aligned} \quad (15)$$

which is of the same form as Equation 5.

Now,

$$V\hat{C}_{21} \cos \hat{\epsilon}_{21} = QC_{21} \cos \epsilon_{21} + RC_{41} \cos \epsilon_{41} \quad (16)$$

$$V\hat{C}_{21} \sin \hat{\epsilon}_{21} = QC_{21} \sin \epsilon_{21} + RC_{41} \sin \epsilon_{41} \quad (17)$$

$$W\hat{C}_{22} \cos \hat{\epsilon}_{22} = SC_{22} \cos \epsilon_{22} + TC_{42} \cos \epsilon_{42} \quad (18)$$

$$W\hat{C}_{22} \sin \hat{\epsilon}_{22} = SC_{22} \sin \epsilon_{22} + TC_{42} \sin \epsilon_{42} \quad (19)$$

Lambeck et al. (1974) have calculated values for the  $C_{k\ell}$  and  $\epsilon_{k\ell}$  from (1) the empirical solution of Dietrich (1944) for the  $K_1$  tide, and (2) from the numerical solution of Bogdanov and Magarik (1967) for the  $S_2$  tide. They are given in Table 2.

If one computes values for Q, R, S, and T from Equations 9, 10, 11, and 12 (using mean orbital elements), and uses the coefficients and phase angles in Table 2, the right hand sides of Equations 16, 17, 18, and 19 can be evaluated. Then, under the assumptions that  $V=Q$  and  $W=S$ , values for  $\hat{C}_{21}$ ,  $\hat{C}_{22}$ ,  $\hat{\epsilon}_{21}$ , and  $\hat{\epsilon}_{22}$  can be computed for each satellite. These are given in Table 3.

These coefficients and phase angles provide a better basis for comparison with those in Table 1. (Unfortunately, no model for the  $P_1$  tide is available for comparison). There is reasonable agreement, except for the  $C_{21}$  for GEOS-I and the  $\epsilon_{22}$  for GEOS-II. Reasons for possible shortcomings in the assumptions made in this work are as follows:

- (1) Inadequacy of the solid Earth tidal model. There is some belief that the Love number  $k_2$  is not a constant for diurnal tides, but is frequency dependent due to core resonance and could introduce errors on the order of 20% in the interpretation of tidal perturbations (McClure (1975)).
- (2) Attributing the total effect, as seen in Figures 3 and 4, to ocean tides alone.
- (3) Inadequacy of the solar atmospheric tidal model for GEOS-II.
- (4) Neglect of higher order coefficients in the solutions.
- (5) Inadequacy of the solar radiation pressure modelling.

We believe, however, that these results indicate the feasibility of recovering global ocean tide parameters from satellite data. This capability will increase as data from more satellites are studied, and as the effects are seen in other of the orbital elements (in particular, the longitude of the ascending node, for which the effects are greater than for the orbital inclination but are more difficult to isolate). The main advantage in using satellite data for recovery of ocean tide parameters lies in the fact that the perturbation due to any tidal constituent appears as a long period effect with a frequency distinctly different from that of any other constituent, whether diurnal or semi-diurnal,

thereby making separation of the constituents quite easy. On the other hand, while surface tidal measurements can be used to separate diurnal from semi-diurnal constituents, it is difficult to differentiate between the various diurnal (or semi-diurnal) constituents unless observations over long periods of time are investigated.

#### **ACKNOWLEDGMENT**

The authors acknowledge the very helpful discussions and suggestions of Bruce Douglas and Ron Williamson in this work.

## REFERENCES

- Anderle, R. , "Refined Geodetic Results Based on Doppler Satellite Observations," Tech. Rept. TR-2889, U.S. Naval Weapons Lab. , Dahlgren, Va. , 1971
- Bogdanov, K. T. , and Magarik, V. A. , "Numerical Solutions for the World's Semi-diurnal ( $M_2$  and  $S_2$ ) Tides," Dokl. Akad. Nauk SSSR, Vol. 172, 1315-1317, 1967
- Chapman, S. , and Lindzen, R. S. , Atmospheric Tides, 200 p. , D. Reidel, Dordrecht, Netherlands, 1970
- Dietrich, G. , "Die Schwingungssysteme der halb-und eintagigen Tiden in den Ozeanen," Veroeff. Meereskunde Univ. Berlin, A41, 7-68, 1944
- Douglas, B. C. , Klosko, S. M. , Marsh, J. G. , and Williamson, R. G. , "Tidal Parameters from the Variation of Inclination of GEOS-I and GEOS-II," Celestial Mechanics, 10, 165-178, 1974
- Douglas, B. C. , Marsh, J. G. , Mullins, N. G. , "Mean Elements of GEOS-I and GEOS-II," Celestial Mechanics 7, 195-204, 1973
- Farrell, W. E. , "Deformation of the Earth by Surface Loads," Rev. Geophys. and Space Phys. , Vol. 10, 761-797, 1972

Jacchia, L. G. , "Static Diffusion Models of the Upper Atmosphere with Empirical Temperature Profiles," SAO Special Report 170, 1965

Jacchia, L. G. , Campbell, I. G. , Slowley, J. W. , "Semi-Annual Density Variations in the Upper Atmosphere, 1958 to 1966," SAO Special Report 265, 1968

Jacchia, L. G. , "New Static Models of the Thermosphere and Exosphere with Empirical Temperature Profiles," SAO Special Report 313, 1970

Jacchia, L. G. , "Revised Static Models of the Thermosphere and Exosphere with Empirical Temperature Profiles," SAO Special Report 332, 1971

Kaula, W. M. , "Celestial Geodesy," in Advances in Geophysics, Vol. 8, Academic Press, New York, 191-293, 1962

Kaula, W. M. , Theory of Satellite Geodesy, Blaisdell Publ. Co. , Waltham, Mass. , 1966

Kaula, W. M. , "Tidal Friction with Latitude Dependent Amplitude and Phase Angle," Astron. J. , Vol. 74, 1108-1114, 1969

Kozai, Y. , "Effects of the Tidal Deformation of the Earth on Close Earth Satellites," Publ. Astron. Soc. Japan, Vol. 17, 395-402, 1965



Kozal, Y. , "Love's Number of the Earth Derived from Satellite Observations," Publ. Astron. Soc. Japan, Vol. 20, 24-26, 1968

Lambeck, K. , Cazenave, A. , and Balmino, G. , "Solid Earth and Ocean Tides Estimated from Satellite Orbit Analyses," Rev. Geophys. and Space Phys., Vol. 12, No. 3, 421-434, 1974

Lerch, F. J. , Wagner, C. A. , Smith, D. E. , Sandson, M. , Brown, J. E. , Richardson, J. A. , "Gravitational Field Models for the Earth (GEM-1 and 2)," NASA TMX-65970, NTIS, Springfield, Virginia, 1972

Longman, I. M. , "Computation of Love Numbers and Load Deformation Coefficients for a Model Earth," Geophys. J. Roy. Astron. Soc., Vol. 11, 133, 1966

Martin, T. V. , "GEODYN Systems Operation Description," Wolf Research and Development Corporation Final Report on Contract NAS 5-11736-129, February 1972

McClure, P. , private communication, 1973

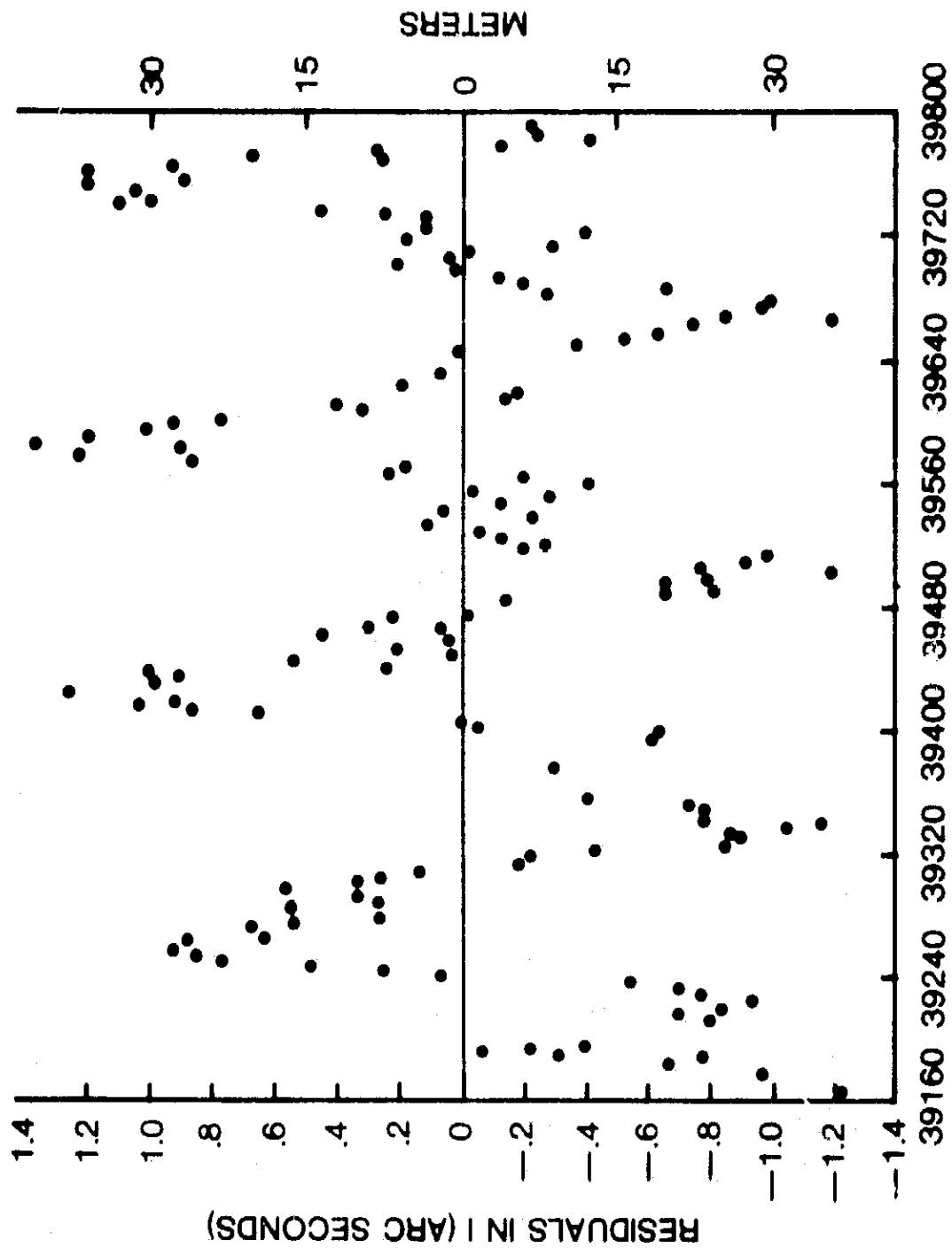
McClure, P. , private communications, 1975

Newton, R. R. , "An Observation of the Satellite Perturbation Produced by the Solar Tide," J. Geophys. Res., Vol. 70, 5983-5989, 1965

Newton, R. R. , "A Satellite Determination of Tidal Parameters and Earth Deceleration," Geophys. J. Roy. Astron. Soc. , Vol. 14, 505-539, 1968

Smith, D. E. , Dunn, P. J. , and Kolenkiewicz, R. , "Earth Tidal Amplitude and Phase," Nature, Vol. 244, 498, 1973

Wagner, C. A. , Douglas, B. C. , Williamson, R. G. , "The ROAD Program," GSFC Document X-921-74-144, 1974



**TIME (MODIFIED JULIAN DATE)**

Figure 1. Perturbation of the GEOS-I Orbit Caused by Solid Earth and Ocean Tides

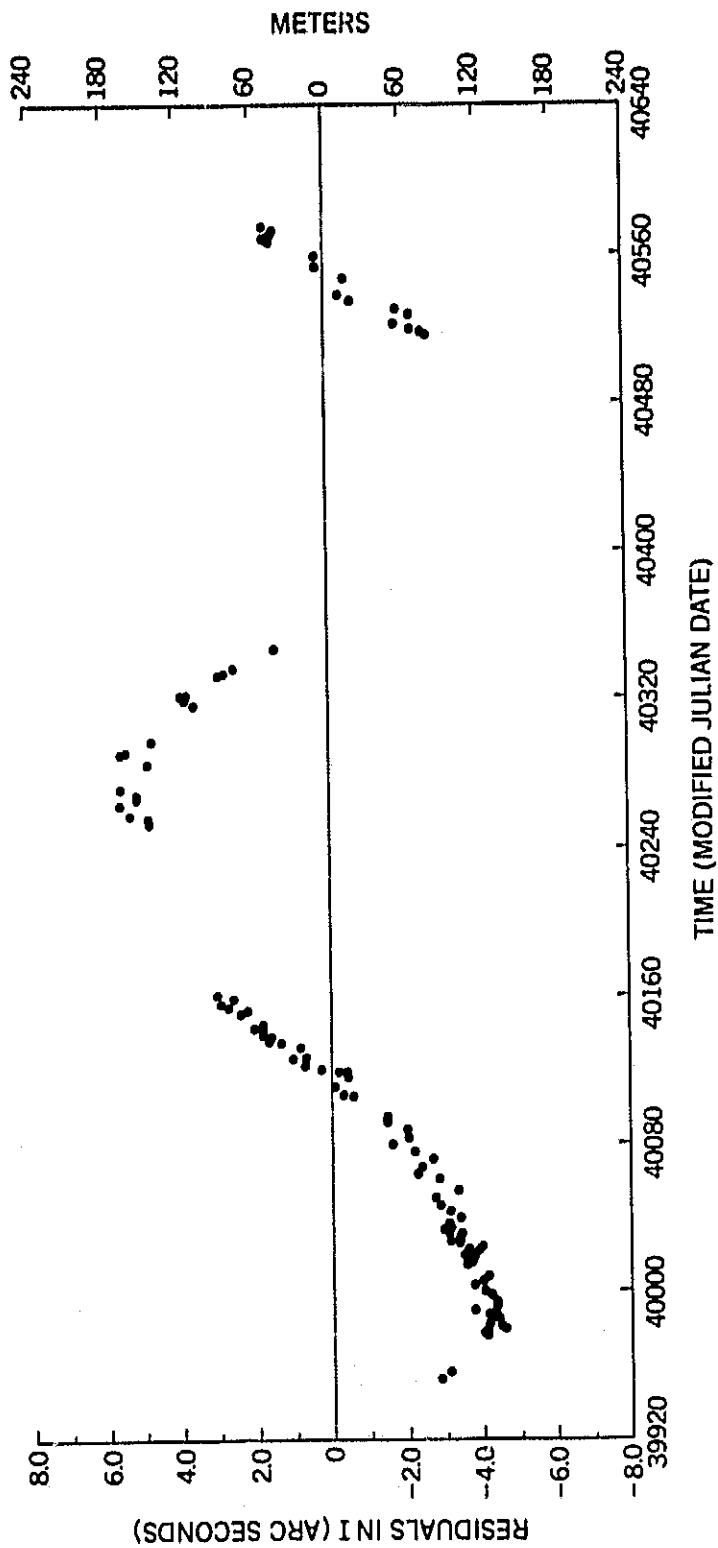


Figure 2. Perturbation of the GEOS-II Orbit Caused by Solid Earth and Ocean Tides

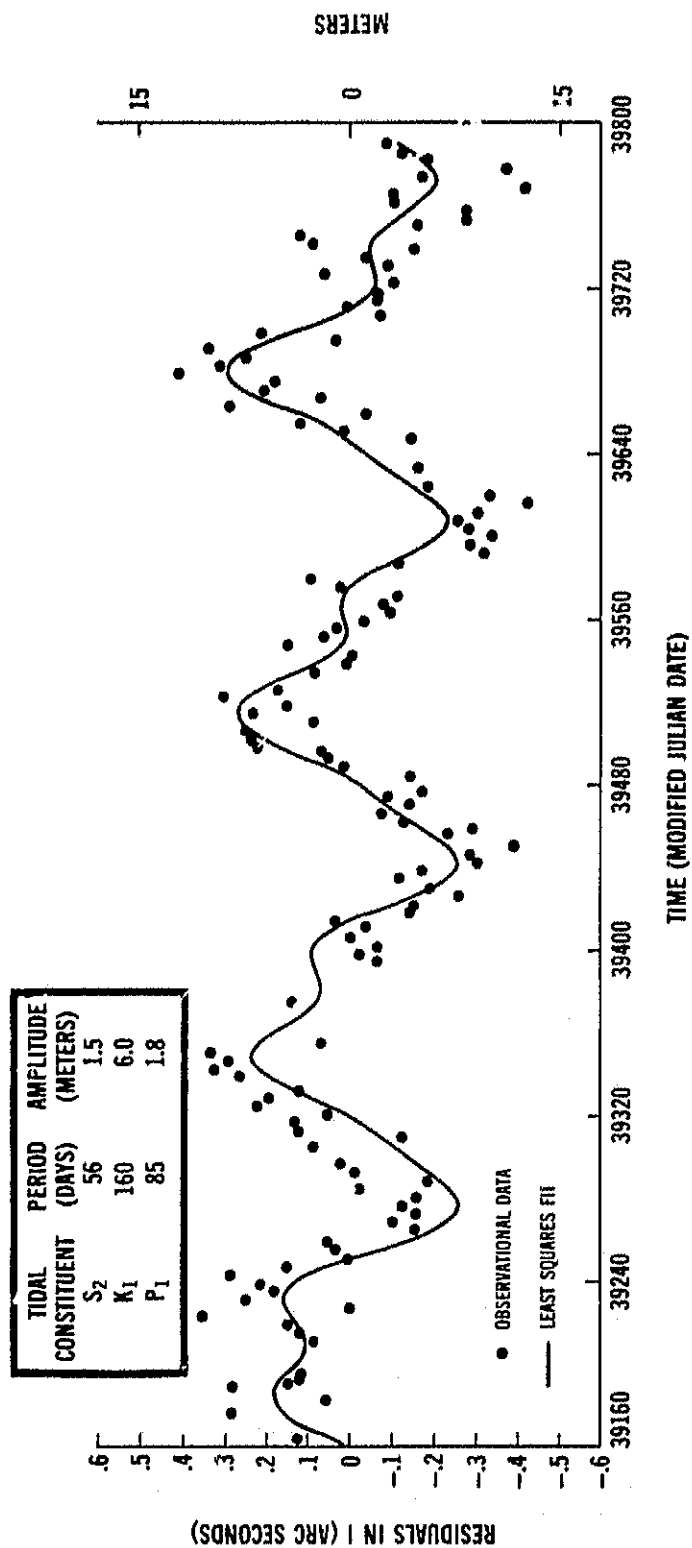


Figure 3. Perturbation of the GEOS-I Orbit Caused by Ocean Tides

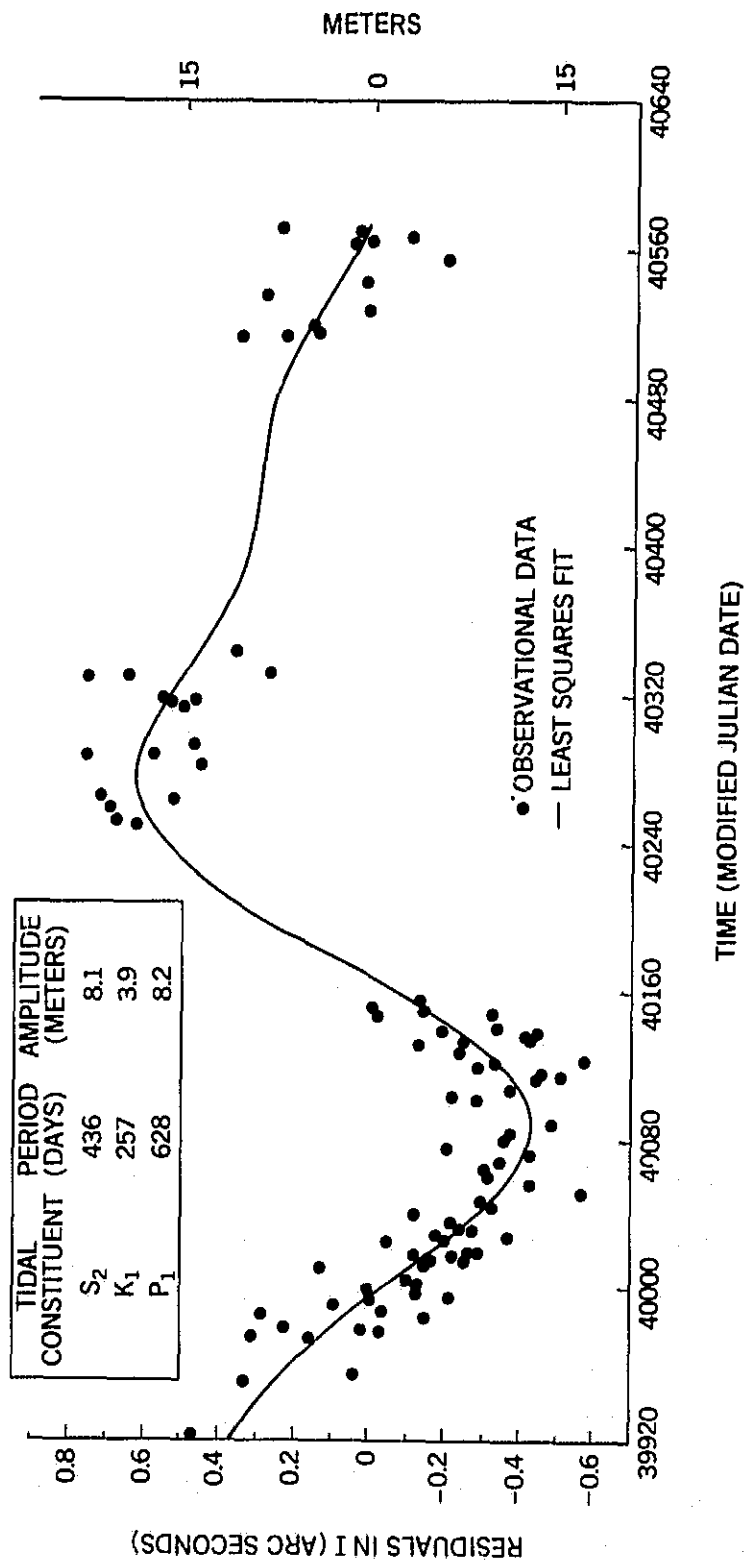


Figure 4. Perturbation of the GEOS-II Orbit Caused by Ocean Tides

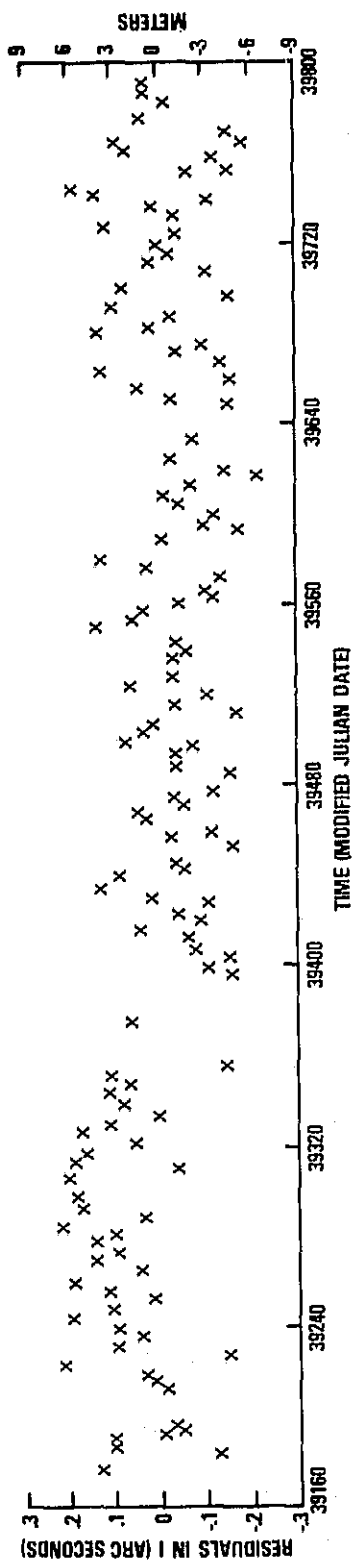


Figure 5. GEOS-I Inclination Residuals After Removal of Tidal Effects

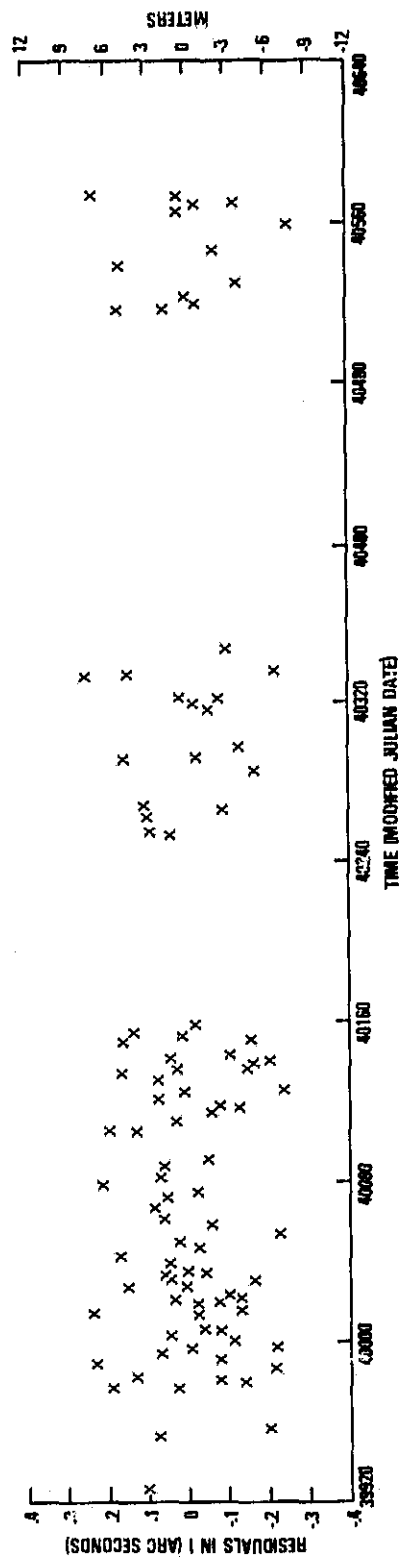


Figure 6. GEOS-II Inclination Residuals After Removal of Tidal Effects

Table 1  
Ocean Tide Parameters Derived from GEOS-I  
and GEOS-II Satellite Observations

Tidal Constituent	Period		Amplitude (Arc Sec)		Coefficient (cm)		Phase	
	GEOS-I	GEOS-II	GEOS-I	GEOS-II	GEOS-I	GEOS-II	GEOS-I	GEOS-II
$S_2$	56d	436d	.05	.27	$1.7 \pm 0.5$	$1.0 \pm 0.2$	$350^\circ \pm 21^\circ$	$62^\circ \pm 11^\circ$
$K_1$	160	257	.20	.13	$8.8 \pm 0.7$	$5.7 \pm 1.6$	$15^\circ \pm 4^\circ$	$334^\circ \pm 15^\circ$
$P_1$	85	628	.06	.27	$5.0 \pm 1.1$	$4.9 \pm 1.1$	$178^\circ \pm 15^\circ$	$127^\circ \pm 12^\circ$

$S_2$  - Solar Semi-diurnal Component

$K_1$  - Combination Luni-solar Diurnal Component

$P_1$  - Solar Diurnal Component



Table 2

## Ocean Tide Parameters from Surface Measurements

<u>Source</u>	<u>Constituent</u>	<u>Coefficients (cm)</u>	<u>Phase Angles</u>
Dietrich (1944)	$K_1$	$C_{21} = 3.3, C_{41} = 1.2$	$\epsilon_{21} = 318^\circ, \epsilon_{41} = 227^\circ$
Bogdanov & Magarik (1967)	$S_2$	$C_{22} = 1.6, C_{42} = 0.2$	$\epsilon_{22} = 310^\circ, \epsilon_{42} = 90^\circ$

Table 3

## Combined Ocean Tide Parameters

<u>Tidal Constituent</u>	<u>Coefficients (cm)</u>		<u>Phase Angles</u>	
	<u>GEOS-I</u>	<u>GEOS-II</u>	<u>GEOS-I</u>	<u>GEOS-II</u>
$K_1$	$\hat{C}_{21} = 4.0$	$\hat{C}_{21} = 5.0$	$\hat{\epsilon}_{21} = 351^\circ$	$\hat{\epsilon}_{21} = 6^\circ$
$S_2$	$\hat{C}_{22} = 1.7$	$\hat{C}_{22} = 1.5$	$\hat{\epsilon}_{22} = 307^\circ$	$\hat{\epsilon}_{22} = 312^\circ$